Dissipative periodic waves, solitons, and breathers of the nonlinear Schrödinger equation with complex potentials

F. Kh. Abdullaev,[1,2] V. V. Konotop,[1,3] M. Salerno,[4] and A. V. Yulin[1]
[1]*Centro de Física Teórica e Computacional, Faculdade de Ciências, Universidade de Lisboa, Avenida Professor Gama Pinto 2, Lisboa 1649-003, Portugal*
[2]*Physical-Technical Institute, Uzbek Academy of Sciences, 2-b G. Mavlyanov Str., 100084 Tashkent, Uzbekistan*
[3]*Departamento de Física, Faculdade de Ciências, Universidade de Lisboa, Campo Grande, Ed. C8, Piso 6, Lisboa 1749-016, Portugal*
[4]*Dipartimento di Fisica "E.R. Caianiello," CNISM and INFN-Gruppo Collegato di Salerno, Università di Salerno, Via Ponte don Melillo, 84084 Fisciano (SA), Italy*
(Received 10 March 2010; published 12 November 2010)

Exact solutions for the generalized nonlinear Schrödinger equation with inhomogeneous complex linear and nonlinear potentials are found. We have found localized and periodic solutions for a wide class of localized and periodic modulations in the space of complex potentials and nonlinearity coefficients. Examples of stable and unstable solutions are given. We also demonstrated numerically the existence of stable dissipative breathers in the presence of an additional parabolic trap.

DOI: 10.1103/PhysRevE.82.056606 PACS number(s): 05.45.Yv, 42.65.Tg, 42.65.Sf

I. INTRODUCTION

Dissipative wave phenomena in nonlinear media with complex parameters are attracting nowadays a great deal of attention. They appear naturally in optics of active media such as, for example, cavities, active fibers, etc. [1] and in quantum mechanics when inelastic interactions of particles with external forces are accounted for [2]. More recently, there has been a particular interest in the dynamics of nonlinear waves in periodic complex potentials due to possible applications to matter waves in absorbing optical lattices [3,4] and to periodic modulations of a complex refractive index in nonlinear optics [5,6]. In this last case special attention was devoted to the so-called *PT* potentials [i.e., complex potentials for which the nonlinear Schrödinger (NLS) equation becomes invariant under the parity and time-reversal symmetry] [7], whose remarkable linear properties are presently intensively investigated [8,9]. In particular, it has been shown that in nonlinear media with *PT*-symmetric *linear* damping and amplifications, stationary localized and periodic states may exist [10]. The stability problem of these nonlinear structures is still an open problem. Also, it is not investigated so far whether similar structures with real energies could also exist in a general complex potential, thanks to the balance between nonlinearity, dispersion, gain, and dissipation.

In the present paper we shall address these problems with a twofold aim. From one side we derive a set of exact soliton solutions of the NLS equation with complex potentials and show that the nonlinearity management technique of the gain-loss profile can be an effective mechanism for providing stability.

We find exact solutions by adopting an inverse engineering approach, developed in [11] for the case of the conservative NLS equation with periodic coefficients. More specifically we assume a specific pattern for the solutions and determine *a posteriori* the potentials which can sustain such pattern as a solution. Using this approach we determine a general class of potentials which may support dissipative periodic waves and solitons in the form of elliptic functions. We show that some of these solutions may be stable with respect to small perturbations.

From the other side, we show that the derived solutions can be used to explore interesting dynamical behaviors of localized modes of the complex NLS equation. To this regard we investigate stable breather solutions which originate from localized exact solutions when a parabolic trap is switched on as additional real potential. Using the strength of the parabolic trap as a parameter we show the occurrence of a bifurcation from an attractor center, corresponding to a stationary soliton, to a limit cycle, corresponding to a stable breather mode.

The stability of stationary periodic solutions, single-hump solitons, and breathers opens the possibility to experimentally observe such waves both in nonlinear optics and in Bose-Einstein condensates (BEC) with optical lattices in the presence of dissipative effects.

We remark that although the determination of the potentials from the solutions is opposite to what usually occurs in practical contexts where potentials are *a priori* fixed, there are physical situations in which an inverse approach can be experimentally implemented. An example of this is the case of Bose-Einstein condensate nonlinear optical lattices which are produced by means of spatial modulations of the interatomic scattering length. In the mean-field approximation the system is described by the NLS equation with spatially modulated nonlinearity of the type considered in this paper. Since the modulation of the scattering length (nonlinearity) in a real experiment is controlled by external magnetic fields via a Feshbach resonance, in principle, one can construct arbitrary potentials to support specific prepared states, implementing thus an inverse engineering approach. Another situation, where the potential can be adjusted in accordance with the profile designed *a priori*, is the nonlinear optics of waveguide arrays, where the thermo-optics effect is employed using heaters producing the temperature gradients properly distributed in space. This gives the hope that some of the exact solutions reported in this paper could be indeed observed in experimental contexts.

The paper is organized as follows. In Sec. II we introduce the model equation and explain the inverse method used to determine the solutions. In Sec. III we apply the method to the case in which there are only linear real and complex potentials. As an example we derive solutions in the potential which has the *PT* symmetry. We show that some of these solutions can be stable, which is confirmed by both the linear stability analysis and numerical time evolutions of the complex NLS equation. In Sec. IV we do similar studies for the case of nonlinear lattices, and we show an example of exact stable solutions in correspondence of more general potentials, while in Sec. V we use this solution to numerically show the existence of dissipative breathers in the complex NLS equation with additional real parabolic trap. Finally, in Sec. VI the main results of the paper are briefly summarized.

II. MODEL AND METHOD

We consider the generalized NLS equation with varying in space complex linear potential, $U_l(x) \equiv V_l(x) + iW_l(x)$, and complex nonlinearity parameter $U_{nl} \equiv V_{nl}(x) + iW_{nl}(x)$ (hereafter, $V = \mathrm{Re}\, U$ and $W = \mathrm{Im}\, U$),

$$i\psi_t = -\tfrac{1}{2}\psi_{xx} + \sigma|\psi|^2\psi + U_l(x)\psi + U_{nl}(x)|\psi|^2\psi, \tag{1}$$

where $\sigma = \pm 1$ and is introduced in an explicit form in order to facilitate transition to the case of the homogeneous nonlinearity [just putting $V_{nl}(x), W_{nl}(x) \equiv 0$]. In the particular case of the *PT* symmetry the invariance imposes restrictions on the linear and complex potentials, namely, V_l, V_{nl} must be even and W_l, W_{nl} must be odd functions of the space variable, respectively.

We will be interested in the solutions of the form $\psi = A(x)\exp\{i[\theta(x) - \omega t]\}$, where $A(x)$ and $\theta(x)$ are real amplitude and inhomogeneous phase of the mode. Substituting this ansatz in Eq. (1) we obtain the system of equations

$$\omega A + \frac{1}{2}A_{xx} - \frac{A}{2}v^2 - \sigma A^3 - V_l A - V_{nl}A^3 = 0, \tag{2}$$

$$A_x v + \frac{1}{2}Av_x - W_l A - W_{nl}A^3 = 0, \tag{3}$$

where $v \equiv \theta_x$.

Let us now assume that linear and nonlinear potentials $V_l(x)$ and $V_{nl}(x)$ are given and pose the problem of designing dissipative terms $W_l(x)$ and $W_{nl}(x)$ to obtain a given solution $A(x)$ [11]. We emphasize that this choice is only for illustration proposes and any pair of the four functions $V_{l,nl}(x)$ and $W_{l,nl}(x)$ can be chosen as *a priori* given.

As the first step, we prove that this is indeed possible, provided that $A(x)$ is a bounded function [13] satisfying the condition

$$|f(x)| < \mathrm{const}, \quad \text{where } f(x) \equiv A_{xx}/A, \tag{4}$$

for all x. Indeed, after dividing Eq. (2) by A we obtain explicit expression for the velocity,

$$v^2(x) = 2(\omega - V_l) + f(x) - 2(\sigma + V_{nl})A^2. \tag{5}$$

As it is clear this equation always has solutions for sufficiently large frequency ω. Next, substituting Eq. (5) in Eq. (3) we find the expression for the dissipative potentials,

$$W_l + W_{nl}A^2 = \frac{1}{2A^2}\frac{d}{dx}(A^2 v) = \frac{A_x v}{A} + \frac{1}{2}v_x. \tag{6}$$

If we want to consider only nonsingular dissipative terms, then we have to impose one more constraint on the field A, which must be considered together with Eq. (4),

$$\left|\frac{A_x v}{A}\right| < \mathrm{const}, \tag{7}$$

and assume v to be a smooth function of x.

In what follows we limit ourselves only by this kind of dissipation. This allows us to indicate immediately several types of admissible solutions:

(i) *Type 1*: A is bounded and has no zeros. These, for example, are functions such as $\mathrm{dn}(x,k)$, etc.

(ii) *Type 2*: A is bounded and has no zeros in any finite domain, but decays as $|x| \to \infty$. These are solutions such as $1/\cosh(x)$, $\exp(-x^2)$, etc.

For these types of solutions condition (7) is automatically satisfied if we restrict our consideration to bounded conservative potentials. Further, we relax the requirements for A allowing it to have zeros, but we require that condition (7) holds. Then condition (4) leads to another type of solutions:

(iii) *Type 3*: A has zeros which coincide with those of A_{xx}. These are solutions of the type $\sim \mathrm{sn}(x,k)$, etc.

All solutions reported below belong to one of these three types. We would like to notice here that A must not necessarily be taken in the form of elliptic functions. We choose elliptical functions just as an example representing periodic solutions with a given parameter (the elliptic modulus). Alternatively we could choose the field A in the form of, for instance, Gaussian function. Another remark we would like to make here is that if A is a solution of the homogeneous NLS equation, then the coefficients V_l and V_{nl} are constants, and one has to determine W_l from either Eq. (3) or Eq. (6) for a chosen W_{nl}. Notice that this procedure implies some freedom, in the sense that one can also think of determining W_{nl} for chosen W_l. However, the latter might require some additional conditions on the linear dissipative potential W_l because sn-like solutions have zeros. In general terms this case is mentioned in the paper as a solution of type 3.

In closing this section we remark that from the above analysis it follows that for all constructed potentials one can define a function $f(x)$ such that the nonlinear solutions are also solutions of the linear problem $A_{xx} - f(x)A = 0$. This observation leads to an immediate interesting conclusion. Assume that $V_{nl}(x) < 0$ and choose $f(x) = -2(\omega - V_l)$. Then, for periodic functions V_l, the solution A is nothing but a *linear Bloch function* of the linear potential $2V_l(x)$. Indeed, in this case $A_{xx} - 2V_l(x)A = -2\omega A$ and $v(x) = \sqrt{2|V_{nl}|}A$, which means that condition (7) is satisfied.

III. CASE OF LINEAR COMPLEX POTENTIALS

According to the scheme described above one can design the dissipation of the system in such a way to provide any desired field configuration supported by the given linear and

nonlinear conservative potentials. While the zoo of available nonlinear patterns is not limited, physically the most relevant cases are those corresponding to the stable solutions. Below we present several examples of the stable field distribution, completing the analysis with a contrasting behavior of unstable patterns.

Before going into detail we also notice that the diversity of the physical parameters at hand makes the analysis of particular cases cumbersome. It turns out, however, that at least one of them can be scaled out. In particular, the amplitude of the nonlinear conservative potential can be scaled out by the renormalization of the amplitude of the solution. Therefore, in what follows this value is chosen to be fixed.

We start the analysis of the particular cases with the natural test example where $A(x)$ is chosen to be a solution of the standard NLS equation, i.e., having constant real linear and nonlinear potentials. We, respectively, set V_l=const and V_{nl}=0. By means of straightforward algebra one obtains, from Eqs. (5) and (6), the relation $W_l(x)=-W_{nl}(x)A^2$. As it is clear this relation includes the particular case $W_l=W_{nl}=0$, which precisely corresponds to the integrable NLS equation. Note, however, that the obtained relation allows for a general class of equations, all having the chosen function $A(x)$ as a solution, and the ratio of the linear and nonlinear complex parts of the potential is fixed to $-A^2(x)$.

Now we turn to the case where $U_l(x)\neq 0$ and $U_{nl}(x)$ is a real constant, which will be chosen to be ± 1, i.e., to the case where the inhomogeneity is only linear and nonlinear gain or loss is absent. The first example is a cnoidal wave (solution of type 3 according to the classification introduced in the previous section),

$$A = A_0\,\mathrm{cn}(x,k), \tag{8}$$

embedded in the linear lattice potential $V_l(x)=V_0\,\mathrm{cn}^2(x,k)$ with a constant focusing nonlinearity $\sigma=-1$. Requiring $\omega=1/2-k^2$, the respective pattern can be created with only the help of the linear dissipative term

$$W_l = -W_0\,\mathrm{sn}(x,k)\mathrm{dn}(x,k), \quad W_0 = \frac{3}{\sqrt{2}}\sqrt{A_0^2 - V_0 - k^2},$$

as it follows from Eq. (6). The hydrodynamic velocity of the obtained solution is given by $v=\sqrt{2}W_0\,\mathrm{cn}(x,k)$. The phase is $\theta=(\sqrt{2}W_0/k)\arccos[\mathrm{dn}(x,k)]$. The obtained complex potential $U_l(x)$ is PT invariant.

As it follows from Eq. (9) the nonlinear pattern $A(x)$ exists only for the amplitudes above the threshold $A_0^{(th)}=\sqrt{V_0+k^2}$ and grows with the intensity of the dissipative part. If $k\neq 0$ then the solution is periodic. However, if $k=1$ then our solution is localized and has no zeros. So if $k=1$ then the solution belongs to type 2. The typical field distributions for solutions are shown in Fig. 1.

Let us now consider the stability of the solutions. To do this we linearize Eq. (1) around the examined soliton solution. The solution of the linearized equation can be sought in the form $\varphi(t,x)=\Sigma_m\varphi_m(x)\exp(\lambda_m t)$. The spectrum λ of the small perturbations has both a continuous part, associated with nonlocalized eigenfunction, and a discrete part, associated with localized modes φ_m. The existence of λ with positive real part means that the corresponding eigenmode will grow exponentially in time and, thus, the examined solution will be unstable. In this paper we study the stability by numerically substituting the spatial derivatives by their discrete analogs (we used five-point approximation). Then the problem of finding the eigenvalues λ governing the stability of the solution is reduced to the diagonalization of a matrix.

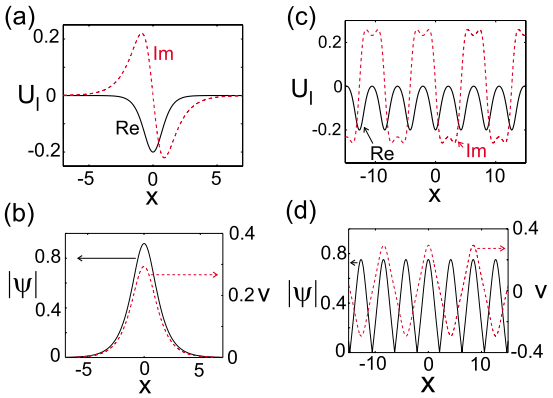

FIG. 1. (Color online) (a) The distributions of the real (solid black curve) and imaginary (dashed red curve) parts of the linear potential given by Eq. (9) for $k=1$ and $A_0=0.92$. (b) The distribution of the amplitude $|\psi|$ (solid black curve, left vertical axis) and the phase gradient v (dashed red curve, right vertical axis) of field ψ. (c) and (d) show the same but for $k=0.85$ and $A_0=0.75$. All panels are for $V_0=-0.2$ and $W_0=0.44$.

Discussing the stability we should first notice that if $V_0=W_0=0$ then Eq. (1) is nothing but the standard NLS equation. The spectrum of small perturbation on the background of the Schrödinger soliton has two pairs of degenerate zero eigenvalues corresponding to phase and translational symmetries. The introduction of a nonzero $U_l(x)$ preserves the phase invariance but breaks the translational symmetry. In Fig. 2 we show the evolution of the eigenvalues in the complex plane as the linear potentials are increased with the ratio V_0/W_0 kept constant.

We see that by increasing the potentials away from zero, the splitting of the zero eigenvalue present at $V_0=W_0=0$ gives a pair of eigenvalues lying in the gap of the continuum, which move in opposite directions along the imaginary axis without producing any instability of the solution. We have therefore that for sufficiently small $U(x)$ the soliton solution is always stable. However, when the pair of the eigenvalues

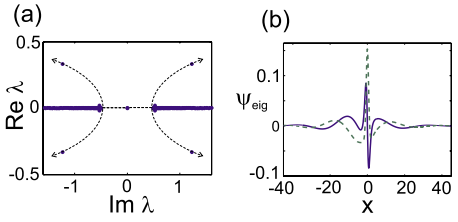

FIG. 2. (Color online) (a) The spectrum for $k=1$, $A_0=1.04$, $V_0=-1$, and $W_0=2.2$ for the case when potentials are given by Eq. (9) and the background solution is given by Eq. (8). The arrows show the direction of the motion of the eigenvalues when $V_{0,l}$ and $W_{0,l}$ increase. (b) The eigenvector of the unstable mode.

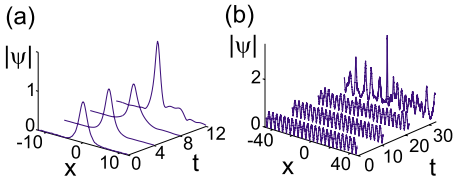

FIG. 3. (Color online) (a) The decay of an unstable solitary solution (8), $A_0=1.04$, $V_0=-1$, $W_0=2.2$, and $k=1$. (b) The decay of an unstable periodical solution, $A_0=0.7$, $V_0=-0.2$, $W_0=0.44$, and $k=0.8$.

reach the border and collide with the continuum, they generate a quartet of complex eigenvalues with two unstable modes generating an oscillatory instability of the soliton.

The development of the instability is illustrated in Fig. 3. Figure 3(a) shows the instability of a soliton with the parameters $V_0=-1$ and $W_0=2.2$. The instability results in an infinitely growing localized peak in the area where the gain is positive. The formation of this peak is clearly seen on the picture. Figure 3(b) shows the decay of a periodic structure because of the instability present at the parameters $V_0=-0.2$ and $W_0=0.44$ (let us mention that at this parameters localized solution is stable). One can see that the instability is of the same kind and results in the formation of growing peaks in the areas of positive gain.

Solution (8) is periodic and describes a pattern with spatially alternating currents, such that the average hydrodynamic velocity is zero (see Fig. 1). It is not difficult to present an example where a pattern corresponds to a nonzero currents. To this end we consider the same wave (8) but now in the potential

$$V_l(x) = V_0\,\mathrm{cn}^2(x,k) - \tilde{V}\,\mathrm{cn}^4(x,k), \tag{9}$$

and require the wave amplitude to be $A_0=\sqrt{V_0+k^2}$ and frequency to be $\omega=1/2-k^2$. This immediately leads to the dissipative part of the potential in the form

$$W_l(x) = -\sqrt{8\tilde{V}}\,\mathrm{sn}(x)\mathrm{cn}(x)\mathrm{dn}(x).$$

Now the hydrodynamic velocity is given by $v(x)=(W_0/2)\mathrm{cn}^2(x,k)$ and the phase is

$$\theta = (W_0/2)E[\mathrm{am}(x,k),k],$$

where $E(x,k)$ is the incomplete elliptic integral of the second kind and $\mathrm{am}(x,k)$ is Jacobi amplitude function. The obtained solutions can be either stable or unstable; the potential and field distributions for a stable solutions are shown in Fig. 4.

Let us now turn to the case of defocusing medium, $\sigma\equiv 1$, and concentrate on the conservative potential in the form $V_l=V_0\,\mathrm{sn}^2(x,k)$. A stable wave can be chosen in the form

$$A = A_0\,\mathrm{dn}(x,k) \tag{10}$$

and is induced by the spatial distributions of the dissipation and losses,

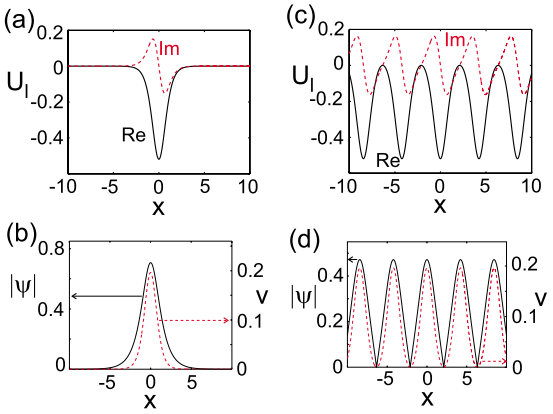

FIG. 4. (Color online) (a) The distributions of the real (solid black curve) and imaginary (dashed red curve) parts of the linear potential given by Eq. (9) for $k=1$ and $A_0=0.71$. (b) The distribution of the amplitude of $|\psi|$ (solid black curve, left vertical axis) and the phase gradient (dashed red curve, right vertical axis) of field ψ given by Eq. (8). (c) and (d) show the same but for $k=0.85$ and $A_0=0.47$. All panels are for $V_0=-0.5$ and $\tilde{V}=0.019$.

$$W_l = -W_0\,\mathrm{sn}(x,k)\mathrm{cn}(x,k),$$

$$W_0^2 = \frac{9k^2}{2}(V_0 - k^2 - k^2A_0^2). \tag{11}$$

One can see that its solution is of type 1. The frequency of the solutions and the hydrodynamic velocity are given by $\omega=V_0/k^2-1+k^2/2$ and $v(x)=(2W_0/3k^2)\mathrm{dn}(x)$. The phase then is readily obtained from the velocity as $\theta(x)=\int_{-\infty}^{x}v(y)dy$. Figure 5 illustrates the potential and the field distribution for a stable solution of such a kind.

IV. CASE OF NONLINEAR COMPLEX POTENTIALS

Let us now turn to the case where the linear potential is absent, i.e., $U_l(x)\equiv 0$, and consider spatially dependent non-

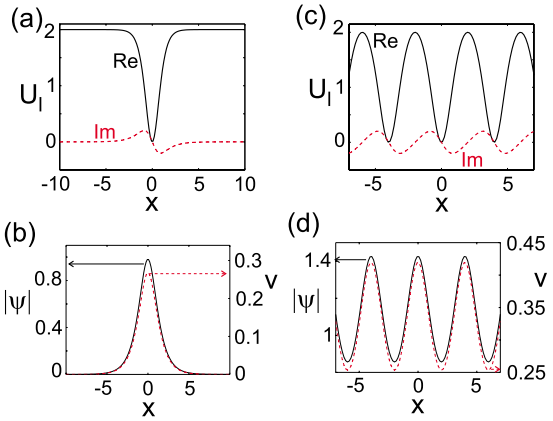

FIG. 5. (Color online) (a) The distributions of the real (solid black curve) and imaginary (dashed red curve) parts of the linear potential given by Eq. (11) for $k=1$ and $A_0=0.98$. (b) The distribution of the amplitude $|\psi|$ (solid black curve, left vertical axis) and the phase gradient v (dashed red curve, right vertical axis) of the field ψ given by Eq. (10). (c) and (d) show the same but for $k=0.8$ and $A_0=1.43$. All panels are for $V_{0,l}=2$ and $W_{0,l}=0.4042$.

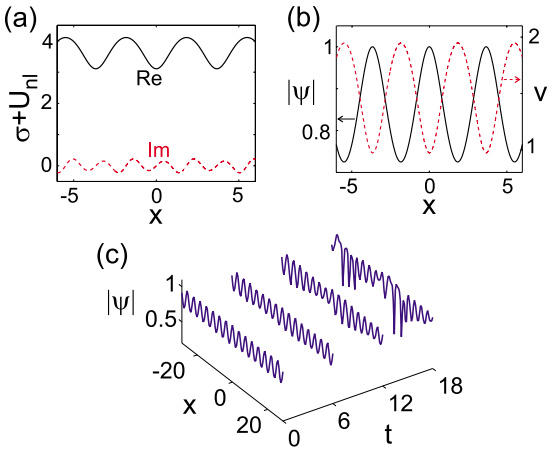

FIG. 6. (Color online) (a) The distributions of the real (solid black curve) and imaginary (dashed red curve) parts of the nonlinear potential given by Eqs. (12) and (13). (b) The distributions of the amplitude $|\psi|$ (solid black curve, left vertical axis) and the phase gradient (dashed red curve, right vertical axis) of the field ψ. (c) The instability developing on the solution (b) perturbed with small noise. All panels are for $k=0.689$.

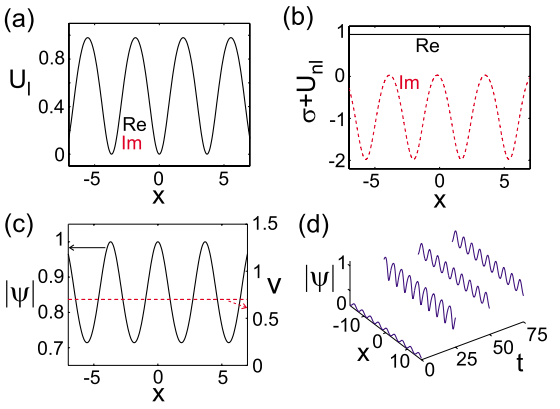

FIG. 7. (Color online) (a) The distributions of the real and imaginary parts of the linear potential given by Eq. (16) for $k=0.7$ (they coincide). (b) The same for the nonlinear potential given by Eq. (17); solid black line is for the real part and dashed red line is for the imaginary part. (c) The distribution of the amplitude $|\psi|$ (solid black curve, left vertical axis) and the phase gradient v (dashed red curve, right vertical axis) of the field ψ. (d) The relaxation of the initial field to the solution shown in (c). All panels are for $a=1$ and $k=0.7$.

linearity. Respectively, it is considered that $V_{nl}(x)$ is given, and the problem to design the dissipative term inducing the given field pattern is posed. Notice that in general the conservative nonlinear part cannot change sign, i.e., the medium cannot be focusing in some regions of the domain and defocusing in others. We consider the case of a defocusing nonlinearity $\sigma=1$ and look for a solution of type (10) with $A_0=1$ (a solution belonging to type 1) embedded in the potential

$$V_{nl}=\frac{1}{k^2}+\mathrm{sn}^2(x,k). \tag{12}$$

Then the hydrodynamic velocity is given by $v(x)=\sqrt{2}k[1+\mathrm{sn}^2(x,k)]$, and imposing the frequency $\omega=3k^2/2+1+1/k^2$ the nonlinear dissipative part is computed from Eq. (6) to be

$$W_{nl}=\frac{\sqrt{2}k\ \mathrm{sn}(x,k)\mathrm{cn}(x,k)}{\mathrm{dn}^3(x,k)}[1-k^2-2k^2\mathrm{sn}^2(x,k)]. \tag{13}$$

The profiles of the nonlinear potential, the distribution of the field, and the development of the instability for solution (16) are shown in Fig. 6.

In the case of *focusing* nonlinearity $\sigma\equiv-1$ we consider mode (8) (belonging to type 3) loaded in the potential

$$V_{nl}(x)=1-\frac{1+k^2}{2A_0^2}+\tilde{V}_{nl}\,\mathrm{cn}^2(x,k) \tag{14}$$

and set $\omega=1/2-k^2/2$. Then, from Eq. (6) we get

$$W_{nl}(x)=-\frac{\sqrt{8\tilde{V}_{nl}}}{A_0}\frac{\mathrm{sn}(x)\mathrm{dn}(x)}{\mathrm{cn}(x)}. \tag{15}$$

The phase is $\theta=\sqrt{2\tilde{V}_{nl}}A_0E[\mathrm{am}(x,k),k]$.

Finally, we consider a more general case when there exists a linear real potential with complex linear and nonlinear inhomogeneous dissipative terms. We let $\sigma\equiv1$ and consider pattern (10) loaded in the linear lattice $V_l(x)=2k^2\,\mathrm{sn}^2(x,k)$. Then requiring $\omega=k^2+1$ we obtain that pattern (10) of type 1 is induced by the distribution of linear and nonlinear dissipative terms as follows:

$$W_l(x)\equiv aV_l(x), \tag{16}$$

$$W_{nl}=-\frac{k^2\ \mathrm{sn}(x,k)}{\mathrm{dn}^3(x,k)}[2a\ \mathrm{sn}(x,k)\mathrm{dn}(x,k)+k\ \mathrm{cn}(x,k)]. \tag{17}$$

The phase is $\theta=kx$ and the velocity field is therefore constant. The potentials and the field distributions for Eqs. (16) and (17) when $a=1$ are shown in Fig. 7. The solution can be stable in its existence $V_{0l}>k^2$ with V_{0l} as the amplitude of the real linear potential. The evolution is shown in Fig. 7(d).

V. DISSIPATIVE BREATHERS

In the limit of infinite period (e.g., for modulus $k=1$) we have that the potentials in Eqs. (16) and (17) give rise to a stable localized hump in the sense that any perturbation of it will relax back to the stationary state. Stable solutions of this type correspond to attractive centers. It is possible to destabilize it into limit cycles and create stable dissipative breathers, by analogy with the bifurcation of a dissipative soliton to a pulsating soliton in the complex Ginzburg-Landau equation [12] (similar studies can be done with other types of soliton solutions given above). We take this solution as the initial condition of the complex NLS with a parabolic trap potential added to the real linear potential, e.g., we take $V_l(x)=\frac{1}{2}\Omega^2x^2+2k^2\,\mathrm{sn}^2(x,k)$, keeping all other potentials the

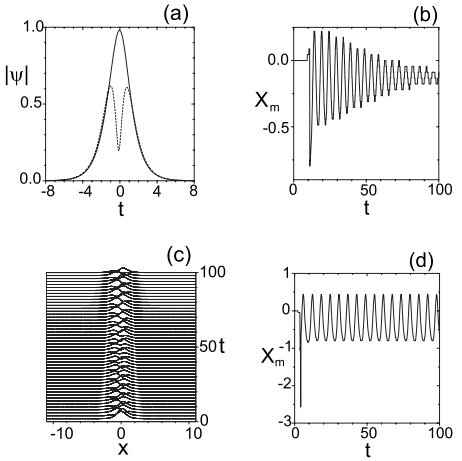

FIG. 8. (a) The modulus of the wave function before ($\Omega=0.05$, continuous line) and after ($\Omega=0.075$, dashed line) the bifurcation. (b) Relaxation of the position of the relative minimum of the density to the new stationary equilibrium. (c) Time evolution of the breathing mode at $\Omega=0.25$. (d) The position of the relative minimum of the density profile versus time during the breather oscillations. All panels are for the same parameter values as in Fig. 7 except for $a=2.0$ and $k=1$.

same. We use the frequency of the parabolic trap as a parameter to induce the transition into a limit cycle. For Ω small enough the extra potential will act as a small perturbation, allowing the solution to relax to a nearby stationary solution of similar shape. We find, however, that when Ω exceeds a critical value, the solution bifurcates from a single-hump to a double-hump shape which is stable and stationary, e.g., it still corresponds to an attractive center. In Fig. 8(a) we show the shapes of the solutions taken before and after the bifurcation, while in Fig. 8(b) we depict the relaxation dynamics of the center of the two-hump solution toward the new equilibrium center. As we increase the strength of the parabolic trap the relaxation time increases until it becomes a regular periodic oscillation [see Fig. 8(d)]. The breather exists in a window in trap frequencies that, for the given parameters, starts at $\Omega_1 \approx 0.2075$ and ends at $\Omega_2 \approx 0.271\,74$. Outside this window the solution returns to be stationary. In Fig. 8(c) we have shown the time evolution of the density profile during the breather motion for a parameter value inside the above existence window.

VI. CONCLUSIONS

Summarizing, we have found the exact solitonic and nonlinear periodic solutions for the generalized NLS equation with complex linear and nonlinear potentials. We have confirmed numerically the stability of some solutions, in particular those having the *PT* symmetry. We have shown that if stable, the solutions are quite robust against perturbations and in this sense they are generic. We have investigated stable breather solutions which originate when a parabolic trap is switched on as additional real potential. Using the strength of the parabolic trap as parameter we have demonstrated that the stationary solutions undergo a bifurcation to a limit cycle which corresponds to a stable breather mode. The stability of both stationary periodic and single-hump soliton solutions and breathers opens the possibility to experimentally observe such waves both in nonlinear optics and in BEC with optical lattices in the presence of dissipative effects.

ACKNOWLEDGMENTS

F.K.A. and V.V.K. were supported by the 7th European Community Framework Programme under Grant No. PIIF-GA-2009-236099 (NOMATOS). A.V.Y. was partially supported by the FCT Grant No. PTDC/EEA-TEL/105254/2008. M.S. acknowledges partial support from MIUR through a PRIN-2008 initiative. This cooperative work was also partially supported by a bilateral project 2009-2010 within the framework of the Portugal (FCT)-Italy (CNR) agreement. Authors are grateful to R. M. Galimzyanov for useful discussions.

[1] I. S. Aranson and L. Kramer, Rev. Mod. Phys. **74**, 99 (2002).
[2] J. G. Muga, J. P. Palao, B. Navarro, and I. L. Egusquiza, Phys. Rep. **395**, 357 (2004).
[3] F. Kh. Abdullaev, A. Gammal, H. L. F. da Luz, and L. Tomio, Phys. Rev. A **76**, 043611 (2007).
[4] Yu. V. Bludov and V. V. Konotop, Phys. Rev. A **81**, 013625 (2010).
[5] Z. H. Musslimani, K. G. Makris, R. El-Ganainy, and D. N. Christodoulides, Phys. Rev. Lett. **100**, 030402 (2008).
[6] K. Staliunas, R. Herrero, and R. Vilaseca, Phys. Rev. A **80**, 013821 (2009).
[7] C. M. Bender and S. Boettcher, Phys. Rev. Lett. **80**, 5243 (1998).
[8] See, e.g., the special issue of J. Phys. A, 39 (2006).
[9] S. Longhi, Phys. Rev. Lett. **103**, 123601 (2009).
[10] Z. H. Musslimani, K. G. Markis, R. El-Ganainy, and D. N. Christodoulides, J. Phys. A **41**, 244019 (2008).
[11] V. A. Brazhnyi and V. V. Konotop, Mod. Phys. Lett. B **18**, 627 (2004).
[12] N. Akhmediev, J. M. Soto-Crespo, and G. Town, Phys. Rev. E **63**, 056602 (2001).
[13] To figure out whether our method could be extended for the case when $A(x)$'s are singular, further investigations are required.